Modern Chemistry
2022; 10(4): 113-120
http://www.sciencepublishinggroup.com/j/mc
doi: 10.11648/j.mc.20221004.12
ISSN: 2329-1818 (Print); ISSN: 2329-180X (Online)

Syntheses, Antioxidant Activity and Crystal Structures of 1-Nicotinoyl-4-Phenylthiosemicarbazide and Its Derivative *N*-Phenyl-5-(Pyridin-3-yl)-1,3,4-Oxadiazol-2-amine

Ndama Faye[1], Aissatou Alioune Gaye[1], Alioune Fall[1], Cheikh Ndoye[1], Mayoro Diop[1], Gregory Excoffier[2], Mohamed Gaye[1, *]

[1]Department of Chemistry, University Cheikh Anta Diop, Dakar, Sénégal

[2]Spectropole, Aix Marseille Université, Marseille, France

Email address:

mohamedl.gaye@ucad.edu.sn (Mohamed Gaye)

[*]Corresponding author

To cite this article:

Ndama Faye, Aissatou Alioune Gaye, Alioune Fall, Cheikh Ndoye, Mayoro Diop, Gregory Excoffier, Mohamed Gaye. Syntheses, Antioxidant Activity and Crystal Structures of 1-Nicotinoyl-4-Phenylthiosemicarbazide and Its Derivative *N*-Phenyl-5-(Pyridin-3-yl)-1,3,4-Oxadiazol-2-amine. *Modern Chemistry*. Vol. 10, No. 4, 2022, pp. 113-120. doi: 10.11648/j.mc.20221004.12

Received: November 23, 2022; **Accepted**: December 7, 2022; **Published**: December 15, 2022

Abstract: The title compound $C_{13}H_{12}N_4OS$ (*I*) is synthetized from nicotinic hydrazide and isothiocynate. Compound $C_{13}H_{10}N_4O$ (*II*) is obtained upon reaction of (*I*) with Mn (II) salt. Compound *I* crystallizes in the triclinic space group $P\bar{1}$ with the following unit cell parameters: a = 9.5667 (2) Å, b = 11.5464 (2) Å, c = 12.6658 (2) Å, α = 78.320 (1)°, β = 83.319 (1)°, γ = 88.079 (2)°, V = 1360.73 (4) Å^3, Z = 4, R_1 = 0.040 and wR_2 = 0.112 and compound *II* crystallizes in the monoclinic space group $P2_1/n$ with the following unit cell parameters: a = 5.4055 (2) Å, b = 19.686 (1) Å, c = 10.5015 (4) Å, β = 92.402 (2)°, V = 1116.51 (8) Å^3, Z = 4, R_1 = 0.070 and wR_2 = 0.212. The asymmetric unit contains two molecules of *I*. For both molecules, the carbonyl oxygen atom and the sulfur atom are, respectively, in *syn* and *trans* conformation with respect to their related amino nitrogen atoms. Strong intermolecular bonds of type N—H···N, N—H···S, and N—H···O, and weak intermolecular bonds of type C—H···O and C—H···S form chains superimposed on each other which are linked, resulting in a three-dimensional network architecture. The heterocyclic compound (*II*) 1,3,4-oxadiazol derivative is not planar with dihedral angle of 17.725 (14)° and 4.550 (15)° between 1,3,4-oxadiazole ring and phenyl and pyridine rings respectively. The dihedral angle between the phenyl and pyridine rings is 22.260 (12)°. In the compound II, intramolecular hydrogen bonds of type C—H···N resulting in *S*(6) ring stabilize the structure. One intermolecular hydrogen bonds of type N—H···N links the molecules thus forming a chain parallel to the *c*-axis.

Keywords: Phenyl Isothiocyanate, Thiosemicarbazide, Hydrazide, Oxadiazole, Antioxidant, Activity

1. Introduction

Phenyl isothiocyanate and hydrazide derivatives have been successfully used in the preparation of numerous compounds which are used in different fields [1–6]. Phenyl isothiocyanate derivatives have been shown to possess antibacterial, antifungal, antitubercular, antithyroid and anticancer properties [7–16]. These compounds possess heteroatoms which can link metal cations resulting in coordination compounds. The metallic derivatives can act as catalyst in numerous organic reactions [17, 18]. Hydrazide derivatives shows biological properties such as antibacterial [19], antitumoral [20], antifungal [21] and spasmolytic activity [22]. Additionally, complexes derived from ligand containing hydrazide moiety can increase their activity. Complexes are also found to be anticancer drug [23], catalyst [24], anti-Alzheimer [25], antimicrobial [26] and antifungal [27]. Phenyl isocyanate and hydrazide are widely used to synthetize thiosemicarbazide derivative [28–30]. Based, on the thiosemicarbazide derivatives, oxadiazole can be synthetized in the presence of metal cation such as Fe(II). Their derivative are promising compounds with a broad spectrum of biological activity in both agrochemical and pharmaceutical field. Oxadiazoles have been shown to possess biological activity such as herbicidal [31], insecticidal [32], hypoglycemia [33], hypotension [34],

antitumor [35] and antimicrobial [36].

We have recently begun to examine the coordination behavior of a series of substituted thiosemicarbazide derivatives that possess a number of interesting properties. In this paper, we report the synthesis and the characterization of a thiosemicarbazide derived from nicotinic hydrazide and phenyl isothiocyanate. In our attempt to synthesize the iron complex from the above derivative, we have isolated 1,3,4-oxadiazole derivative. The two molecules are characterized by spectroscopic study and X-ray diffraction technic.

2. Experimental Part

2.1. Starting Materials and Instrumentation

Isonicotinic hydrazide, phenyl isothiocynate, iron chloride tetrahydrate and manganese acetate tetrahydrate were purchased from Sigma-Aldrich and used as received without further purification. All solvents used were of reagent grade. Elemental analyses of C, H and N were recorded on a VxRio EL Instrument. Infrared spectra were obtained on a FTIR Spectrum Two of Perkin Elmer spectrometer in the 4000-400 cm^{-1} region.

2.2. Synthesis of 1-nicotinoyl-4-phenylthiosemicarbazide (I)

For the synthesis of 1-nicotinoyl-4-phenylthiosemicarbazide I, a mixture of nicotinic hydrazide (0.01 mol) and phenyl isothiocynate (0.01 mol) in absolute ethanol was refluxed for 12 h. The solid material obtained on cooling was filtered, washed with diethyl ether, air-dried.

Yield: 87%. Elemental Anal. $C_{13}H_{12}N_4OS$, Found (Calcd.) (%): C, 57.34 (57.32); H, 4.44 (4.41); N, 20.57 (20.53); S, 11.77 (11.72). IR (ν, cm^{-1}): 3212, 3110 (N-H), 1681 (C=O), 1444 (N—N), 1256 (C=S), 753 cm^{-1}, 688 cm^{-1}. ^1H NMR (DMSO-d_6, δ(ppm)): 10.80 (S, 1H, NH), 9.82 (S, 1H, NH), 9.77 (S, 1H, NH), 8.75-7.30 (m, 9H, Ar-H). ^{13}C NMR (DMSO-d_6, δ(ppm)): 120-150, 164.85, 181.11.

2.3. Synthesis of N-phenyl-5-(pyridin-3-yl)-1,3,4-oxadiazol-2-amine (II)

For the synthesis of II, a stirred mixture of (I) (272.3 mg, 1 mmol) and $FeCl_2 \cdot 4H_2O$ (198.8 mg, 1 mmol) in ethanol was refluxed for 2 h. After cooling, the solution was filtered off and the precipitate was then crystallized from a methanol. Yield 58%. Elemental Anal. $C_{13}H_{10}N_4O$, Found (Calcd.) (%): C, 65.54 (65.52); H, 4.23 (4.21); N, 23.52 (23.51). IR (ν, cm^{-1}): 1568, 1560, 1497, 1444, 1159, 830, 790, 754, 685, 678, 515.

2.4. X-ray Crystallography

Crystals suitable for X-diffraction, of the reported compound, were grown by slow evaporation of MeOH solution of the complex. Details of the X-rays crystal structure solution and refinement are given in Table 1. Diffraction data were collected using a SuperNova Rigaku Oxford Diffraction with graphite monochromatized Cu *Kα* radiation (λ = 1.54184 Å). All data were corrected for Lorentz and polarization effects. No absorption correction was applied. Complex scattering factors were taken from the program package SHELXTL [37]. The structures were solved by direct methods which revealed the position of all non-hydrogen atoms. All the structures were refined on F2 by a full-matrix least-squares procedure using anisotropic displacement parameters for all non-hydrogen atoms [38]. The hydrogen atoms were geometrically optimized and refined as riding model by AFIX instructions. Molecular graphics were generated using ORTEP-3 [39].

2.5. DPPH Free Radical Scavenging

Antioxidant capacities of compound (I) was measured according to Akhtar et al. [40] with modifications. 3.8 mL of the methanol solution of DPPH· (40 mg/L) was added to test compound (200 μL) at different concentrations. The mixture was shaken vigorously and incubated in dark for 30 min at room temperature. After the incubation time, the absorbance of the solution was measured at 517 nm by using UV-vis spectrophotometer Perkin two. The DPPH· radical scavenger effect was calculated using the Equation (1):

$$Scavenging\ activity\ (\%\ control) = \frac{Absorbance_{control} - Absorbance_{sample}}{Absorbance_{control}} \times 100$$

where $A_{control}$ is the absorbance of the control reaction and A_{sample} is the absorbance of the test compound. The tests were carried out in triplicate. Trolox was used as positive control.

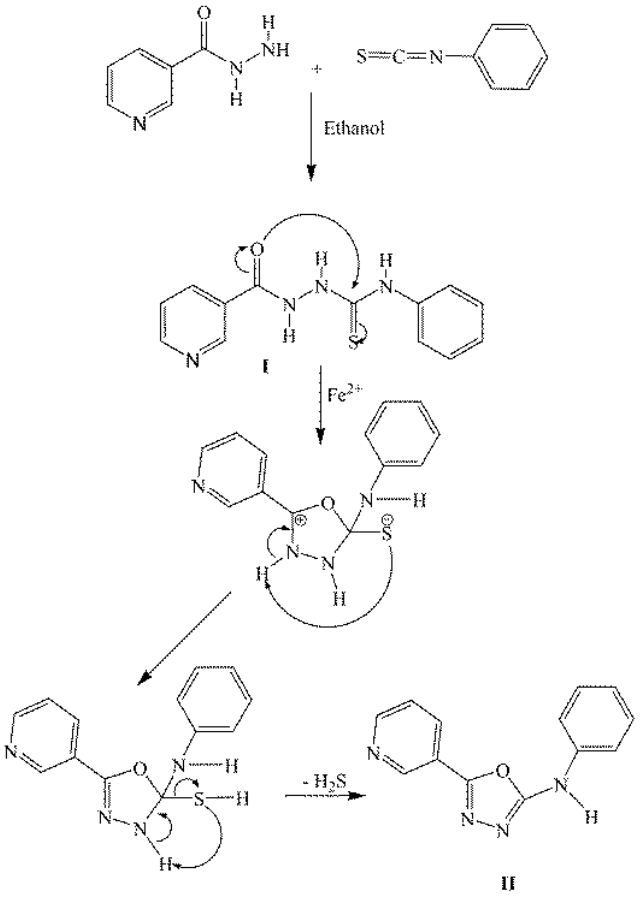

Figure 1. *Synthetic routes of I and II.*

Table 1. *Experimental details.*

Chemical formula	**$C_{13}H_{12}N_4OS$**	**$C_{13}H_{10}N_4O$**
M_r	272.33	238.25
Crystal system, space group	Triclinic, $P\bar{1}$	Monoclinic, $P2_1/n$
Temperature (K)	295	293
a, b, c (Å)	9.5667 (2), 11.5464 (2), 12.6658 (2)	5.4055 (2), 19.686 (1), 10.5015 (4)
α, β, γ (°)	78.320 (1), 83.319 (1), 88.079 (2)	90.00, 92.402 (4), 90.00
V (Å^3)	1360.73 (4)	1116.51 (8)
Z	4	4
Radiation type	Cu $K\alpha$	Cu $K\alpha$
μ (mm^{-1})	2.10	0.78
Crystal size (mm)	0.26 × 0.14 × 0.03	0.24 × 0.11 × 0.08
No. of measured, independent and observed [$I > 2\sigma(I)$] reflections	26994, 5452, 5103	4543, 2148, 1817
R_{int}	0.034	0.026
R [$F^2 > 2\sigma(F^2)$], $wR(F^2)$, S	0.040, 0.112, 1.07	0.070, 0.212, 1.08
No. of reflections	5452	2148
No. of parameters	343	163
$\Delta\rho_{max}$, $\Delta\rho_{min}$ (e Å^{-3})	0.40, −0.34	0.42, -0.28

3. Results and Discussion

3.1. Spectroscopic Study

The NMR spectra of compound I are recorded in dmso-d_6. The ^{1}H NMR spectrum shows characteristic signals at 10.80 ppm, 9.82 ppm and 9.77 ppm. attributed to the three N—H moieties present in the molecule. The signals due to the aromatic protons are in the rang 7.30-8.75 ppm. The ^{13}C NMR spectrum exhibits two signals at 181.11 ppm and 164.85 ppm characteristic of C=S and C=O, respectively [41]. Additional signals attributed to the aromatic carbon atoms are pointed in the range 150-140 ppm. The infrared spectrum of compound I exhibited characteristic bands. The bands of medium intensities appearing at 3212 cm^{-1} and 3110 cm^{-1} are attributed to N—H stretching vibration. The bands pointed at 1681 cm^{-1} is attributed to the C=O linked to the pyridyl ring. The band due to the N—N and C=S moieties are respectively pointed at 1444 cm^{-1} and 1256 cm^{-1}. Additional band pointed in the regions 1600-1400 cm^{-1} are attributed to the phenyl and the pyridyl ring. Bands at 753 cm^{-1} and 688 cm^{-1} are indicative of the presence of monosubstituted aromatic rings. Upon reaction of I with Fe(II), the organic compound II is isolated. The infrared spectrum of II is strongly different from the spectrum of I. The FTIR of II present bands due to aromatic rings. Bands at 1159 cm^{-1} and 1444 cm^{-1} are attributed to the oxadiazole C—O—C and the N—N moieties, respectively [42]. Crystals suitable for X-ray determination were grown from slow evaporation of methanol solution of I and II.

3.2. X-ray Structures Determination

3.2.1. Structure of 1-nicotinoyl-4-phenylthiosemicarbazide (I)

The molecular structure of compound I with the atomic label shown in Figure 2. The asymmetric unit contains two independent molecules of 1-nicotinoyl-4-phenylthiosemicarbazide (Figure 2). The Thiosemicarbazide moieties [N1—C7(S1)—N2—N3 and N1A—C7A(S1A)—N2A—N3A] are almost planar with rms of 0.0186 Å and 0.0998 Å, respectively. For one of the molecule present in the asymmetric unit, the thiosemicarbazide moiety forms dihedral angles of 82.684(10)° and 85.919 (10)° with the phenyl and pyridyl rings, respectively, while the phenyl ring and the pyridyl ring form dihedral angle of 49.994 (11)°. For the second molecule, the thiosemicarbazide moiety forms dihedral angles of 49.511(10)° and 83.196(10)° with the phenyl and pyridyl rings, respectively, while the phenyl ring and the pyridyl ring form dihedral angle of 58.994(12)°. The distances C=O and C=S are slightly different in the two molecules (C1=O1 [1.209 (2) Å], C7=S1 [1.7091 (14) Å) and (C1A=O1A [1.2194 (18) Å], C7A=S1A [1.6837 (14) Å]).

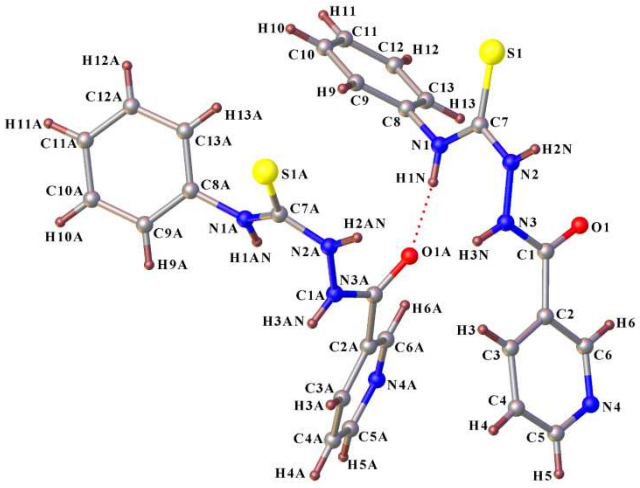

Figure 2. *Crystal structure of 1-nicotinoyl-4-phenylthiosemicarbazide (I).*

The values of these bonds lengths which are compatible with double bond character, shows that the compound did not undergo enolization or thioenolization as observed for similar molecules [43, 44]. The molecules of the compound are exclusively in their keto/thioketo form. This form is confirmed by the C1—N3 [1.360 (2) Å], C7—N2 [1.3399 (19) Å], C7—N1 [1.3223 (19) Å], C1A—N3A [1.3494 (18) Å], C7A—N2A [1.3654 (18) Å] and C7A—N1A [1.3286 (18) Å] distances, which indicate that these are single bonds

[45, 46]. Other distances and angles are the same magnitude in the two molecules present in the asymmetric unit. The O1 and N2 atoms are in *syn* conformation with respect to C1—N3 [O1—C1—N3—N2 = -12.1(3)°] while S1 and N3 atoms are in *trans* conformation with respect to C7—N2 [S1—C7—N2—N3 = -177.0(1)°]. Similar conformations are observed for the second molecule with torsions angles of 3.6(2)° [O1A—C1A—N3A—N2A] and 161.4(1)° [S1A—C7A—N2A—N3A]. The two molecules are linked by intramolecular hydrogen bond of type N—H···O between the amino group of one molecule which acts as donor and a carbonyl oxygen atom of the other molecule which acts as acceptor (N1—H1N···O1A), resulting in a dimer (Figure 2). The Figure 3 shows the overlay of the two molecules in the asymmetric unit. In the crystal, in addition to the strong intermolecular bonds of type N—H···N, N—H···S, and N—H···O, the structure features weak intermolecular bonds of type C—H···O and C—H···S. The structure consists of several chains superimposed on each other. These chains are linked by intermolecular bonds which ensure the cohesion and stability of the polymer. The combined hydrogen bonds links give rise to a three-dimensional network architecture (Figure 4).

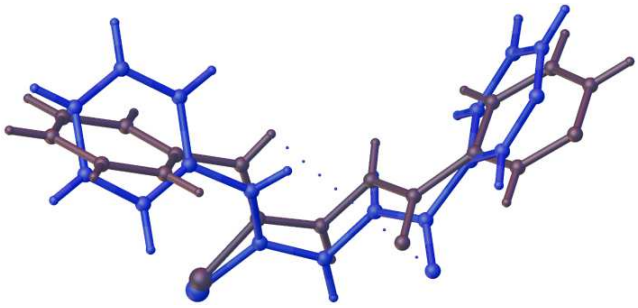

Figure 3. *Overlay of the two independent similar molecules present in the asymmetric unit of I.*

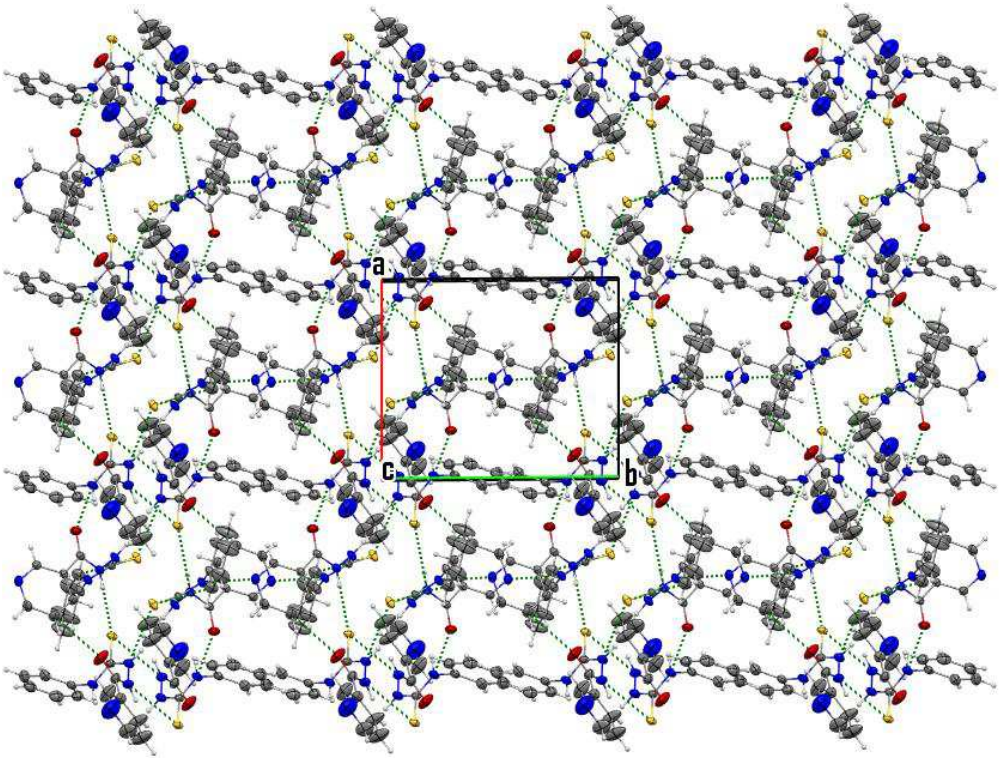

Figure 4. *Crystal packing of I observed along the c-axis.*

Table 2. *Selected geometric parameters (Å, °).*

S1—C7	1.7091 (14)	N2A—C7A	1.3654 (18)
S1A—C7A	1.6837 (14)	N3—C1	1.360 (2)
O1A—C1A	1.2194 (18)	N3—N2	1.3920 (17)
N1A—C7A	1.3286 (18)	N2—C7	1.3399 (19)
N3A—C1A	1.3494 (18)	N1—C7	1.3223 (19)
N3A—N2A	1.3895 (16)	O1—C1	1.209 (2)
N1A—C7A—N2A	116.75 (12)	N1—C7—N2	119.04 (13)
N1A—C7A—S1A	125.08 (11)	N1—C7—S1	122.56 (11)
N2A—C7A—S1A	118.17 (10)	N2—C7—S1	118.36 (11)
O1A—C1A—N3A	123.65 (13)	O1—C1—N3	121.07 (16)
O1A—C1A—C2A	122.47 (13)	O1—C1—C2	122.63 (17)
N3A—C1A—C2A	113.80 (12)	N3—C1—C2	116.30 (14)

Table 3. *Hydrogen-bond geometry (Å, °).*

D—H···*A*	*D*—H	H···*A*	*D*···*A*	*D*—H···*A*
N1A—H1AN···N4A^{i}	0.86	2.10	2.8527(17)	145.7
N3A—H3AN···S1^{ii}	0.86	2.57	3.3183(13)	145.7
N2A—H2AN···S1^{iii}	0.86	2.66	3.4435(13)	152.8
N3—H3N···S1^{iii}	0.86	2.62	3.3450(14)	142.6
N2—H2N···S1A^{iii}	0.86	2.49	3.2310(14)	144.7
N1—H1N···O1A	0.86	2.04	2.8213(17)	150.8
C4A—H4A···O1^{ii}	0.93	2.34	3.094(2)	138.0
C9A—H9A···S1^{ii}	0.93	2.99	3.719(2)	135.9
C5—H5···S1A^{iv}	0.93	2.97	3.838(2)	155.1

Symmetry codes: (i) −x+1, −y+1, −z+1; (ii) x+1, y, z; (iii) −x, −y, −z+1; (iv) x, y, z+1

3.2.2. Structure of N-phenyl-5-(pyridin-3-yl)-1,3,4-oxadiazol-2-amine (II)

Compound II crystallizes in the monoclinic space group P21/n. The asymmetric unit contains one molecule of *N*-phenyl-5-(pyridin-4-yl)-1,3,4-oxadiazol-2-amine (Figure 4). The central 1,3,4-oxadiazol ring C1/N1/N2/C7/O1 is almost planar [rms 0.0067 Å] with short distances C1=N2 [1.278 (3) Å] and C7=N3 [1.302 (3) \%A] indicating double-bond character. The distances C1—O1 [1.379 (2) \%A] and C7—O1 [1.361 (2) Å] are compatible with single-bond character. These values are in accordance with those reported for compound with 1,3,4-oxadiazol moiety [47]. The molecular structure of II is not planar. In fact, the phenyl and pyridine rings form dihedral angles of 17.725(14)° and 4.550(15)°, respectively, with the central five-membered ring 1,3,4-oxadiazole ring. The dihedral angle between the phenyl and the pyridine rings is 22.260(12)°. The oxadiazole molecule is stabilized by the intramolecular C9–H9···N3 hydrogen bonds forming the usual six-membered *S*(6) ring, as shown in Figure 4 (Table 4). There is only one intermolecular hydrogen bond of type N–H···N between the amino group as donor and the pyridine ring nitrogen atom as acceptor, (N4—H4···N1^{i}, i = −*x*+2, −*y*+1, −*z*+1) (Table 4) which propagates to forms chains that extend parallel to the *c*-axis (Figure 5).

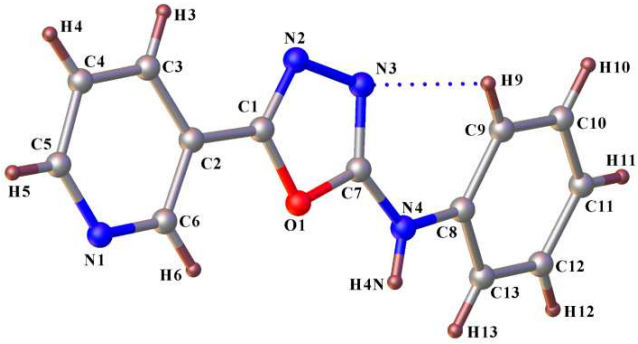

Figure 5. *Crystal structure of N-phenyl-5-(pyridin-3-yl)-1,3,4-oxadiazol-2-amine (II).*

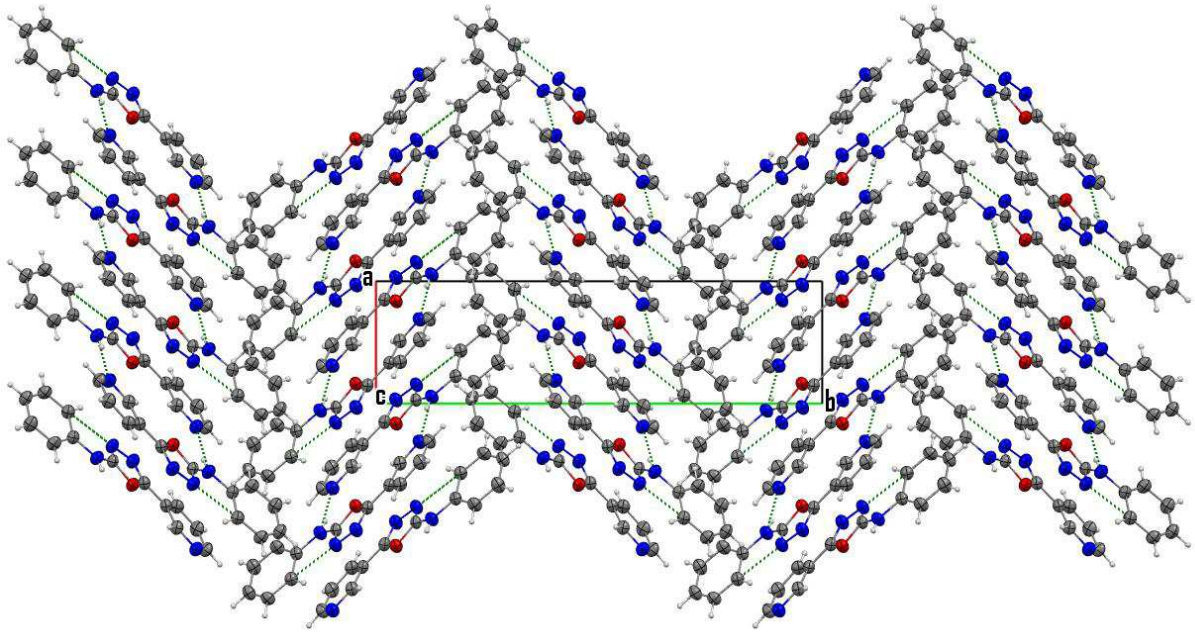

Figure 6. *Crystal packing of II observed along the c-axis.*

Table 4. *Selected geometric parameters (Å, °).*

O1—C1	1.379 (2)	N4—C8	1.404 (3)
O1—C7	1.361 (2)	N4—C7	1.350 (3)
N2—N3	1.413 (3)	N3—C7	1.302 (3)
N2—C1	1.278 (3)	N1—C6	1.322 (3)
O1—C1—C2	118.22 (18)	N4—C7—O1	115.46 (18)
N2—C1—O1	112.16 (19)	N3—C7—O1	113.16 (19)
N2—C1—C2	129.61 (19)	N3—C7—N4	131.4 (2)

Table 5. *Hydrogen-bond geometry (Å, °).*

D*—H···*A	***D*—H**	**H···*A***	***D*···*A***	***D*—H···*A***
N4—H4···N1^{i}	0.86	2.10	2.950 (3)	170.8
C9—H9···N3	0.93	2.40	2.995 (3)	121.9

Symmetry code: (i) −*x*+2, −*y*+1, −*z*+1.

3.3. Antioxidant Activity of Compound I

The method of scavenging the DPPH· radical is used to evaluate the antioxidant activity of organic or inorganic compounds [48, 49]. The antioxidant activity of the compound I has been substantially investigated. Figure 7 shows the plots of DPPH· free radical scavenging activity (%) for Trolox and compound I. The DPPH· is a stable free radical and becomes a stable molecule when it accepts an electron or hydrogen radical. In this study the compound I scavenge the DPPH· radical by hydrogen donating ability. The scavenging activity increases with increasing the concentration in the range tested (100-500 mmol/L). Compound I have scavenging activity between 17.46±0.21 and 79.28±0.66% within the

investigated concentration range due to the three NH groups which can react with DPPH· radical by the typical H-abstraction reaction. When increasing the concentration (100 to 500 mM), the scavenging activity of compound I increases more rapidly than that of Trolox (9.86±0.67-49.66±0.28%).

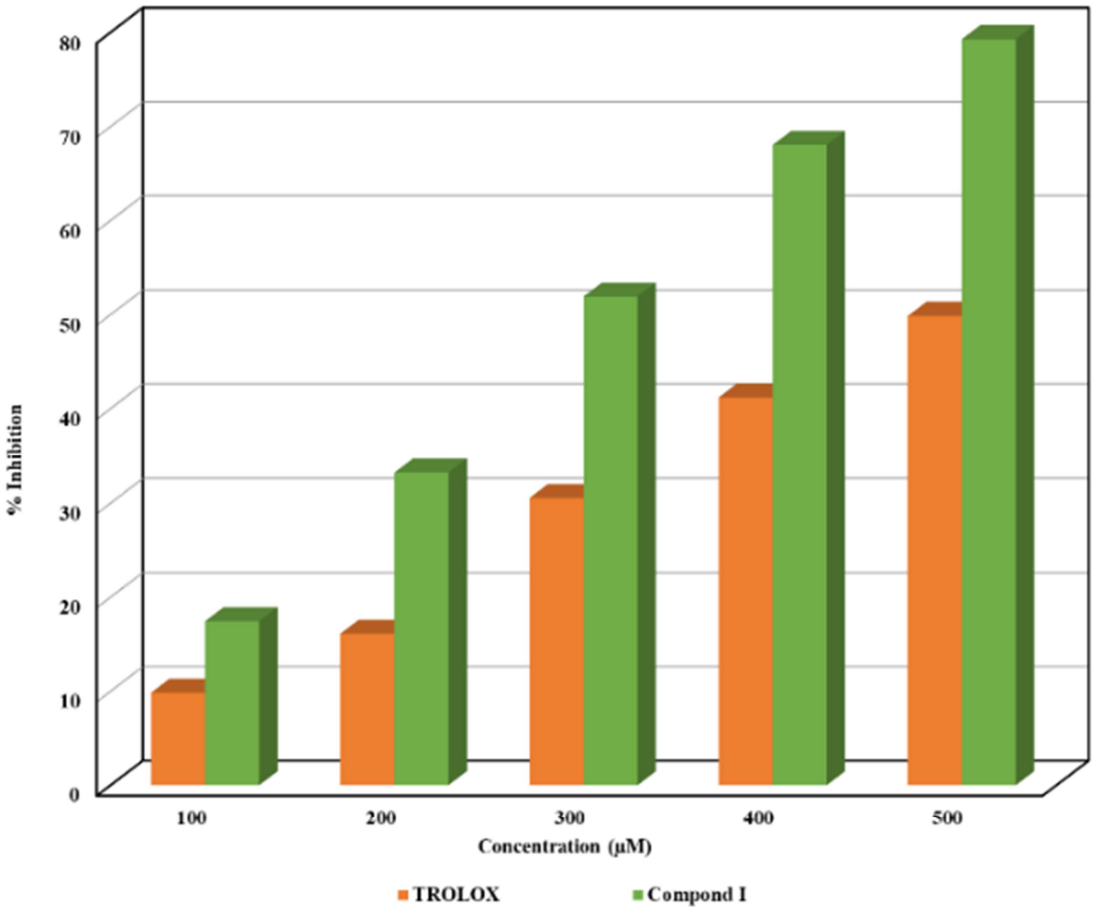

Figure 7. *Antioxidant activity of (I) and Trolox.*

4. Conclusion

Compound, 1-nicotinoyl-4-phenylthiosemicarbazide (I), synthesized from the reaction between nicotinic hydrazide and isothiocynate yields compound II, *N*-phenyl-5-(pyridin-3-yl)-1,3,4-oxadiazol-2-amine, when it reacts with Fe(II). The structures of compounds I and II are confirmed by elemental analysis and spectroscopic techniques (FT-IR, ^{1}H and ^{13}C NMR). The molecular structures of compounds I and II are determined by X-ray diffraction. In the concentration range (100-500 mM) compound I shows better antioxidant power comparatively to that of TROLOX, which is used as a reference.

Supplementary Materials

CCDC- 2221176 and 2221177 contain the supplementary crystallographic data for compounds *I* and *II* respectively. These data can be obtained free of charge via https://www.ccdc.cam.ac.uk/structures/, or by e-mailing data_request@ccdc.cam.ac.uk, or by contacting The Cambridge Crystallographic Data Centre, 12 Union Road, Cambridge CB2 1EZ, UK; fax: +44(0)1223-336033.

References

[1] Jastrzębska, A., Piasta, A., Krzemiński, M. & Szłyk, E. Application of 3,5-bis-(trifluoromethyl)phenyl isothiocyanate for the determination of selected biogenic amines by lc-tandem mass spectrometry and ^{19}F NMR. Food Chemistry, 2018, 239, 225–233. https://doi.org/10.1016/j.foodchem.2017.06.100

[2] Klikarová, J., Česlová, L. & Fischer, J. Rapid analysis of phenyl isothiocyanate derivatives of amino acids present in czech meads. Journal of Chromatography A, 2021, 1644, 462134. https://doi.org/10.1016/j.chroma.2021.462134

[3] Thiruvangoth, S. & Thayyil, M. S. A Comparative study of bacterial activity of allyl isothiocyanate, phenyl isothiocyanate, and 2-(4-hydroxy phenyl) ethyl isothiocyanate using density functional theory. Materials Today: Proceedings, 2022, 55, 102–108. https://doi.org/10.1016/j.matpr.2021.12.401

[4] Guda, D. R., Cho, H. M. & Lee, M. E. Mild and convenient one-pot synthesis of 2-amino-1,3,4-oxadiazoles promoted by trimethylsilyl isothiocyanate (TMSNCS). RSC Adv., 2013, 3 (21), 7684–7687. https://doi.org/10.1039/C3RA41044G

[5] Vytla, D., Emmadi, J., Velayuthaperumal, R., Shaw, P., Cavallaro, C. L., Mathur, A. & Roy, A. Visible-light enabled one-pot three-component petasis reaction for synthesis of α-substituted secondary sulfonamides/amides/hydrazides. Tetrahedron Letters, 2022, 106, 154055. https://doi.org/10.1016/j.tetlet.2022.154055

[6] Wang, J., Xu, W., Qian, J., Wang, Y., Hou, G., Suo, A. & Ma, Y. Injectable hyaluronan/MnO_2 nanocomposite hydrogel constructed by metal-hydrazide coordinated crosslink mineralization for relieving tumor hypoxia and combined phototherapy. Journal of Colloid and Interface Science, 2022, 628, 79–94. https://doi.org/10.1016/j.jcis.2022.08.024.

[7] Lin, C.-M., Preston, J. F., III & Wei, C.-I. Antibacterial mechanism of allyl isothiocyanate. Journal of Food Protection, 2000, 63 (6), 727–734. https://doi.org/10.4315/0362-028X-63.6.727

[8] Takahashi, H., Nakamura, A., Fujino, N., Sawaguchi, Y., Sato, M., Kuda, T. & Kimura, B. Evaluation of the antibacterial activity of allyl isothiocyanate, clove oil, eugenol and carvacrol against spoilage lactic acid bacteria. LWT, 2021, 145, 111263. https://doi.org/10.1016/j.lwt.2021.111263

[9] Quiles, J. M., Nazareth, T. D., Luz, C., Luciano, F. B., Mañes, J. & Meca, G. Development of an antifungal and antimycotoxigenic device containing allyl isothiocyanate for silo fumigation. Toxins, 2019, 11 (3). https://doi.org/10.3390/toxins11030137

[10] Wu, T.-L., Hu, Y.-M., Sun, Y., Zhang, Z.-J., Wu, Z.-R., Zhao, W.-B., Tang, C., Du, S.-S., He, Y.-H., Ma, Y., Yang C.-J. & Liu Y.-Q. Insights into the mode of action of 2-(4-methoxyphenyl)ethyl isothiocyanate on Aspergillus Niger. Food Control, 2022, 136, 108871. https://doi.org/10.1016/j.foodcont.2022.108871

[11] Hearn, M. J., Chen, M. F., Cynamon, M. H., Wang'ondu, R. & Webster, E. R. Preparation, and properties of new antitubercular thioureas and thiosemicarbazides. Journal of Sulfur Chemistry, 2006, 27 (2), 149–164. https://doi.org/10.1080/17415990600576826

[12] Hearn, M. J., Webster, E. R. & Cynamon, M. H. Preparation, and properties of antitubercular 1-piperidino-3-arylthioureas. Journal of Heterocyclic Chemistry, 2005, 42 (6), 1225–1229. https://doi.org/10.1002/jhet.5570420632

[13] Theunis, M., Naessens, T., Peeters, L., Brits, M., Foubert, K. & Pieters, L. Optimization and validation of analytical rp-hplc methods for the quantification of glucosinolates and isothiocyanates in Nasturtium Officinale R. Br and Brassica Oleracea. LWT, 2022, 165, 113668. https://doi.org/10.1016/j.lwt.2022.113668

[14] Ahmed, A., Shafique, I., Saeed, A., Shabir, G., Saleem, A., Taslimi, P., Taskin Tok, T., Kirici, M., Üç, E. M. & Hashmi, M. Z. Nimesulide linked acyl thioureas potent carbonic anhydrase i, ii and α-glucosidase inhibitors: design, synthesis and molecular docking studies. European Journal of Medicinal Chemistry Reports, 2022, 6, 100082. https://doi.org/10.1016/j.ejmcr.2022.100082

[15] Tarar, A., Peng, S., Cheema, S. & Peng, C.-A. Anticancer activity, mechanism, and delivery of allyl isothiocyanate. bioengineering, 2022, 9 (9). https://doi.org/10.3390/bioengineering9090470

[16] Hsu, S.-Y., Lee, S.-C., Liu, H.-C., Peng, S.-F., Chueh, F.-S., Lu, T.-J., Lee, H.-T. & Chou, Y.-C. Phenethyl isothiocyanate suppresses the proinflammatory cytokines in human glioblastoma cells through the PI3K/Akt/NF-KB signaling pathway in vitro. oxidative medicine and cellular longevity, 2022, 2022, 2108289. https://doi.org/10.1155/2022/2108289

[17] Narvariya, R., Das, S., Jain, A. & Panda, T. K. Synthesis, structural characterization and catalytic application of zinc and cadmium sulfur complexes with imidazol-2-ylidene-*N*'-phenylthiourea ligand scaffold. Polyhedron, 2022, 225, 116055. https://doi.org/10.1016/j.poly.2022.116055

[18] Ali Mohammed Al-Ahmed, Z. Novel Cr(III), Ni(II), and Zn(II) complexes of thiocarbamide derivative: synthesis, investigation, theoretical, catalytic, potentiometric, molecular docking and biological studies. Arabian Journal of Chemistry, 2022, 15 (9), 104104. https://doi.org/10.1016/j.arabjc.2022.104104

[19] Mavrikaki, V., Pagonis, A., Poncin, I., Mallick, I., Canaan, S., Magrioti, V. & Cavalier, J.-F. Design, synthesis and antibacterial activity against pathogenic mycobacteria of conjugated hydroxamic acids, hydrazides and O-alkyl/O-acyl protected hydroxamic derivatives. Bioorganic & Medicinal Chemistry Letters, 2022, 64, 128692. https://doi.org/10.1016/j.bmcl.2022.128692

[20] Han, M. İ., Atalay, P., Tunç, C. Ü., Ünal, G., Dayan, S., Aydın, Ö. & Küçükgüzel, Ş. G. Design and synthesis of novel (*S*)-naproxen hydrazide-hydrazones as potent vegfr-2 inhibitors and their evaluation in vitro/in vivo breast cancer models. Bioorganic & Medicinal Chemistry, 2021, 37, 116097. https://doi.org/10.1016/j.bmc.2021.116097

[21] Popiołek, Ł., Tuszyńska, K. & Biernasiuk, A. Searching for novel antimicrobial agents among hydrazide-hydrazones of 4-iodosalicylic acid. Biomedicine & Pharmacotherapy, 2022, 153, 113302. https://doi.org/10.1016/j.biopha.2022.113302

[22] Berillo, D. A. & Dyusebaeva, M. A. Synthesis of hydrazides of heterocyclic amines and their antimicrobial and spasmolytic activity. Saudi Pharmaceutical Journal, 2022, 30 (7), 1036–1043. https://doi.org/10.1016/j.jsps.2022.04.009

[23] Ashma, A., Yahya, S., Subramani, A., Tamilarasan, R., Sasikumar, G., Askar Ali, S. J., Al-Lohedan, H. A. & Karnan, M. Synthesis of new nicotinic acid hydrazide metal complexes: potential anti-cancer drug, supramolecular architecture, antibacterial studies and catalytic properties. Journal of Molecular Structure, 2022, 1250, 131860. https://doi.org/10.1016/j.molstruc.2021.131860

[24] Tuna, M. & Ugur, T. Synthesis of novel of Mn(II), Co(II), and Cu(II) Schiff base complexes and their high catalytic effect on bleaching performance with H_2O_2. Journal of Molecular Structure, 2022, 1265, 133348. https://doi.org/10.1016/j.molstruc.2022.133348

[25] Qurrat-ul-Ain, Abid, A., Lateef, M., Rafiq, N., Eijaz, S. & Tauseef, S. Multi-activity tetracoordinated pallado-oxadiazole thiones as anti-inflammatory, anti-alzheimer, and anti-microbial agents: structure, stability and bioactivity comparison with pallado-hydrazides. Biomedicine & Pharmacotherapy, 2022, 146, 112561. https://doi.org/10.1016/j.biopha.2021.112561

[26] Devi, J., Kumar, S., Kumar, D., Jindal, D. K. & Poornachandra, Y. Synthesis, characterization, in vitro antimicrobial and cytotoxic evaluation of Co(II), Ni(II), Cu(II) and Zn(II) Complexes derived from bidentate hydrazones. Research on Chemical Intermediates, 2022, 48 (1), 423–455. https://doi.org/10.1007/s11164-021-04602-8

[27] Mallikarjuna, B. P., Sastry, B. S., Suresh Kumar, G. V., Rajendraprasad, Y., Chandrashekar, S. M. & Sathisha, K. Synthesis of new 4-isopropylthiazole hydrazide analogs and some derived clubbed triazole, oxadiazole ring systems – a novel class of potential antibacterial, antifungal and antitubercular agents. European Journal of Medicinal Chemistry, 2009, 44 (11), 4739–4746. https://doi.org/10.1016/j.ejmech.2009.06.008

[28] Rogalewicz, B., Climova, A., Pivovarova, E., Sukiennik, J., Czarnecka, K., Szymański, P., Szczesio, M., Gas, K., Sawicki, M., Pitucha, M. & Czylkowska, A. Antitumor activity and physicochemical properties of new thiosemicarbazide derivative and its Co(II), Ni(II), Cu(II), Zn(II) and Cd(II) complexes. Molecules, 2022, 27 (9). https://doi.org/10.3390/molecules27092703

[29] Tokmajyan, G. G. & Karapetyan, L. V. Synthesis and chemical transformations of 2-imino-2,5-dihydrofurans. chemistry of heterocyclic compounds, 2022, 58 (8), 371–383. https://doi.org/10.1007/s10593-022-03101-x

[30] Nguyen, H. H., Pham, Q. T., Phung, Q. M., Le, C. D., Pham, T. T., Pham, T. N. O. & Pham, C. T. Syntheses, structures, and biological activities of Pd(II) and Pt(II) complexes with some 1-picolinoyl-4-substituted thiosemicarbazides. Journal of Molecular Structure, 2022, 1269, 133871. https://doi.org/10.1016/j.molstruc.2022.133871

[31] Zou, X.-J., Lai, L.-H., Jin, G.-Y. & Zhang, Z.-X. Synthesis, fungicidal activity, and 3D-QSAR of pyridazinone-substituted 1,3,4-oxadiazoles and 1,3,4-thiadiazoles. J. Agric. Food Chem., 2002, 50 (13), 3757–3760. https://doi.org/10.1021/jf0201677

[32] Holla, B. S., Gonsalves, R. & Shenoy, S. Synthesis, and antibacterial studies of a new series of 1,2-bis(1,3,4-oxadiazol-2-yl)ethanes and 1,2-bis(4-amino-1,2,4-triazol-3-yl)ethanes. European Journal of Medicinal Chemistry, 2000, 35 (2), 267–271. https://doi.org/10.1016/S0223-5234(00)00154-9

[33] Hamdani, S. S., Khan, B. A., Ahmed, M. N., Hameed, S., Akhter, K., Ayub, K. & Mahmood, T. Synthesis, crystal structures, computational studies, and α-amylase inhibition of three novel 1,3,4-oxadiazole derivatives. Journal of Molecular Structure, 2020, 1200, 127085. https://doi.org/10.1016/j.molstruc.2019.127085

[34] Tyagi, M. & Kumar, A. Synthesis of 2-[2′-Carbomyl-5′-(heteroarylinomethylene)-1′,3',4′-thiadiazol-2′-yl/Oxadiazol-2′-yl)]-4,5-dihydroimidazolines as hypotensive agents. Oriental Journal of Chemistry, 2002, 18 (1).

[35] Fray, M., ELBini-Dhouib, I., Hamzi, I., Doghri, R., Srairi-Abid, N., Lesur, D., Benazza, M., Abidi, R. & Barhoumi-Slimi, T. Synthesis, characterization, and in vivo antitumor effect of new α,β-unsaturated-2,5-disubstituted-1,3,4-oxadiazoles. Synthetic Communications, 2022, 52 (6), 849–860. https://doi.org/10.1080/00397911.2022.2053993

[36] Abdelfattah, A. M., Mekky, A. E. M. & Sanad, S. M. H. Synthesis, antibacterial activity and in silico study of new bis(1,3,4-oxadiazoles). Synthetic Communications, 2022, 52 (11–12), 1421–1440. https://doi.org/10.1080/00397911.2022.2095211

[37] Sheldrick, G. M. SHELXT – Integrated space-group and crystal-structure determination. Acta Crystallographica Section A, 2015, 71 (1), 3–8. https://doi.org/10.1107/S2053273314026370

[38] Sheldrick, G. M. Crystal structure refinement with SHELXL. Acta Crystallographica Section C, 2015, 71 (1), 3–8. https://doi.org/10.1107/S2053229614024218

[39] Farrugia, L. J. WinGX and ORTEP for Windows: an update. Journal of Applied Crystallography, 2012, 45 (4), 849–854. https://doi.org/10.1107/S0021889812029111.

[40] Akhtar, P., Yaakob, Z., Ahmed, Y., Shahinuzzaman, M. & Hyder, M. K. M. Total phenolic contents and free radical scavenging activity of different parts of jatropha species. Asian Journal of Chemistry, 2018, 30, 365–370

[41] Nassar, I. F., Att-Allah, S. R. & Hemdan, M. M. Utility of thiophene-2-carbonyl isothiocyanate as a precursor for the synthesis of 1,2,4-triazole, 1,3,4-oxadiazole and 1,3,4-thiadiazole derivatives with evaluation of their antitumor and antimicrobial activities. Phosphorus, Sulfur, and Silicon and the Related Elements, 2018, 193 (10), 630–636. https://doi.org/10.1080/10426507.2018.1487435

[42] Bondock, S., Adel, S., Etman, H. A. & Badria, F. A. Synthesis and antitumor evaluation of some new 1,3,4-oxadiazole-based heterocycles. European Journal of Medicinal Chemistry, 2012, 48, 192–199. https://doi.org/10.1016/j.ejmech.2011.12.013

[43] Samb, I., Gaye, N., Sylla-Gueye, R., Thiam, E. I., Gaye, M. & Retailleau, P. Crystal structure of *N, N*'-[(ethane-1,2-diyl)bis(azanediylcarbonothioyl)]bis-(benzamide). Acta Crystallographica Section E, 2019, *75* (5), 642–645. https://doi.org/10.1107/S205698901900495X

[44] Sylla-Gueye, R., Thiam, I. E., Orton, J., Coles, S. & Gaye, M. Crystal structure of N'-[4-(dimethylamino)benzylidene]furan-2-carbohydrazide monohydrate. Acta Crystallographica Section E, 2020, 76 (5), 660–663. https://doi.org/10.1107/S205698902000465X

[45] Jian, F.-F. & Li, Y. 1-(4-Hydroxybenzylidene)-4-phenylthiosemicarbazide. Acta Crystallographica Section E, 2006, 62 (10), o4563–o4564. https://doi.org/10.1107/S1600536806037573

[46] Feizi, S., Rezayan, A. H., Sardari, S. & Notash, B. (*E*)-1-(2-Nitrobenzylidene)-4-phenylthiosemicarbazide. Acta Crystallographica Section E, 2012, 68 (7), o2154. https://doi.org/10.1107/S1600536812026803

[47] Lakshmithendral, K., Archana, K., Saravanan, K., Kabilan, S. & Selvanayagam, S. Crystal structures of 3-methoxy-4-{[5-(4-methoxyphenyl)-1,3,4-oxadiazol-2-yl]methoxy}benzonitrile and *N*-(4-{[5-(4-chlorophenyl)-1,3,4-oxadiazol-2-yl]methoxy}phenyl)acetamide. Acta Crystallographica Section E, 2018, 74 (12), 1919–1922. https://doi.org/10.1107/S2056989018016754

[48] Foti, M. C., Daquino, C. & Geraci, C. Electron-transfer reaction of cinnamic acids and their methyl esters with the DPPH· radical in alcoholic solutions. J. Org. Chem., 2004, 69 (7), 2309–2314. https://doi.org/10.1021/jo035758q

[49] Taha, Z. A., Ajlouni, A. M., Momani, W. A. & Al-Ghzawi, A. A. Syntheses, characterization, biological activities and photophysical properties of lanthanides complexes with a tetradentate Schiff base ligand. Spectrochimica Acta Part A: Molecular and Biomolecular Spectroscopy, 2011, 81 (1), 570–577. https://doi.org/10.1016/j.saa.2011.06.052